Lee, B. S., Nix, A. R., & McGeehan, J. P. (2001). A spatio-temporal ray launching propagation model for UMTS pico and microcellular environments. In IEEE VTC Spring 2001, Rhodes, May. (Vol. 1, pp. 367 - 371). Institute of Electrical and Electronics Engineers (IEEE). 10.1109/VETECS.2001.944866

A Spatio-Temporal Ray Launching Propagation Model for UMTS Pico and Microcellular Environments

B.S. Lee, A.R. Nix and J.P. McGeehan
Center for Communication Research, University of Bristol
Merchant Venturers Building, Woodland Road, Bristol, BS8 1UB, UK
Tel: +44 (0)117 9545202, Fax: +44 (0)117 9545206, Email: B.S.Lee@bristol.ac.uk

Abstract

In this paper a new ray-launching algorithm is presented that builds on earlier image based research models. The algorithm has been developed to meet the advanced propagation needs of third and fourth generation networks. New features are incorporated to model unrestricted multiple reflection, transmission and diffraction in three-dimensional pico and microcellular environments. The model simulates full indoor/outdoor interaction, in addition to dedicated indoor or outdoor modelling modes. Results are shown to compare well with wideband microcellular measurements taken in the 2GHz UMTS band.

1. Introduction

An accurate understanding of the radio channel has become vital given the growth of advanced spatial and temporal signal processing techniques at the base station and mobile terminal. Accurate propagation data is now critical in the planning and deployment of spectrally efficient radio systems. Factors such as precise building geometry must be included if accurate power-delay and power-azimuth predictions are to be obtained in microcells. Alternatively, measurement campaigns can be used to obtain detailed spot data, however specialized and expensive equipment is required. The time scales and manpower requirements for such campaigns are also prohibitive when planning the locations of thousands of microcells. Hence, powerful and accurate propagation models are required for pico and microcellular environments.

Currently, most cellular networks are planned using statistical propagation models (occasionally supported by simple ray optics). These models are optimized for signal coverage (power) prediction. In this paper the proposed model predicts power-delay and power-azimuth profiles in addition to signal coverage. Spatial information enables the impact of fixed or adaptive antenna patterns to be determined. This level of prediction also enables new radio architectures (including the use of Space-Time Coding and BLAST) to be assessed under realistic channel conditions.

The propagation model presented in this paper is based on the principles of ray launching. In section 2, a detailed description of the path search engine is presented. This section also explains the ray launching method and the use of reception spheres, or angular information, to determine rays arriving at the receiver. The general modelling approach and the techniques used to support off-axis diffracted rays and irregular terrain are also discussed. The 2GHz measurement system and the microcellular test site are briefly presented in section 3. In section 4, power delay profile predictions are compared with those taken using the Medav channel sounder. Finally, section 5 introduces a number of conclusions and highlights areas of future work.

2. The Ray Launching Technique: Basic Model Theory

Deterministic ray based propagation models generally use one of two key path-searching techniques: (i) ray tracing or (ii) ray launching. Such methods have been used for many years with references dating back to the early 1980s [1-5].

Ray tracing is a technique based on the electromagnetic theory of images. It considers all objects as potential reflectors and calculates the location of transmitter images. Ray paths are formed based on the location of the receiver, the transmitter and its associated images. Ray launching, on the other hand, sends out test rays at a number of discrete angles from the transmitter. The rays interact with objects present in the environment as they propagate. The propagation of a ray is terminated when its power falls below a preset threshold. Both methods have been expanded to enable transmission and diffraction to be considered in the model.

Figure 1 illustrates two common methods by which received paths are deemed to have occurred. In the first method, a propagation distance dependent reception sphere is used. A path from the transmitter to the receiver exists if a ray intersects this reception sphere. The second method uses angular information at the image, or virtual transmitter, to determine if a ray path exists. A path is found if the azimuth and elevation angles of the test path at the virtual transmitter are close enough (within an

0-7803-6728-6/01/$10.00 ©2001 IEEE.

acceptable error bound) to the azimuth and elevation angles of the ray. The geometry of the test path is shown in Figure 1b. The location of the virtual transmitter is determined by reverse propagating the ray by an amount equivalent to the unfolded path length. The ray launching mechanism at the transmitter is clearly linked to the method used at the receiver to determine ray path existence.

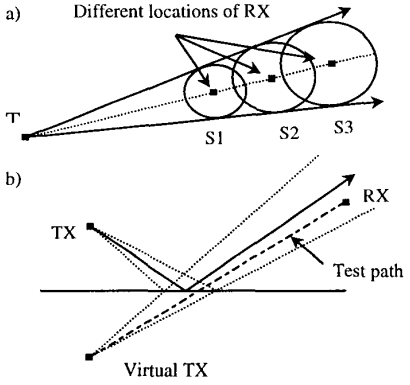

Figure 1: Methods used to determine a path from the transmitter (TX) to the receiver (RX). a) The use of distance dependent reception spheres. b) The use of the angular information at the virtual transmitter (reflected ray path exists between TX and RX).

If reception spheres are used then rays must be uniformly spaced to ensure that no more than three rays touch any given reception sphere. A common method that achieves this requirement is to launch rays such that they pass through the vertices of a unit geodesic sphere enclosing the transmitter. A geodesic sphere is constructed by tessellating the faces of a regular polyhedron and projecting the vertices to the surface of a unit sphere [6].

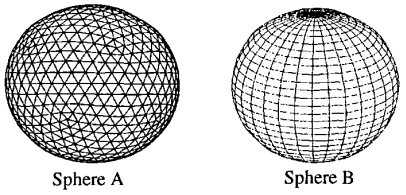

Figure 2: Rays launched from the transmitter pass through the vertices of sphere A if reception spheres are employed, otherwise sphere B is used.

If angular information at the virtual transmitter is to be used then rays must be uniformly spaced in the azimuth and elevation planes. Figure 2 shows the two different launching spheres around the transmitter.

The ray launching technique has a number of advantages when compared with image based ray-tracing methods. Using image theory, the number of images increase significantly as additional reflecting surfaces are introduced (i.e. the use of complex geographic databases). Ray launching methods do not suffer from this problem, however they do posses alternative shortcomings. Ray launching suffers from resolution problems and care must be taken to prevent the double counting of single ray paths. Ray launching is unable to calculate the exact paths as identified using an image based method. Increasing the number of launched rays at the transmitter minimizes the resolution problem. However, this approach will increase the overall computational complexity. Double counting of a single path is an inherent problem when using reception spheres to detect received paths. A common remedy is to apply additional filtering to remove the extra paths, since repeated rays will have the same path length and arrival angle.

The complex electric field, E_i, associated with the i-th ray path is determined by:

$$E_i = E_o f_{ti} f_{ri} \{ \prod_j \overline{\overline{R}}_j \prod_k \overline{\overline{T}}_k \prod_l \overline{\overline{D}}_l A_l(s_l, s_l') \} \frac{e^{-j\beta d}}{d} \qquad (1)$$

where E_o represents the reference field, f_{ti} and f_{ri} the transmitting and receiving antenna field radiation patterns, R_j the reflection coefficient for the j-th reflection, T_k the transmission coefficient for the k-th transmission, D_l the diffraction coefficient and A_l the diffraction spatial attenuation given the $1/d$ dependence for the l-th diffraction and $e^{-j\beta d}$ the propagation phase factor ($\beta=2\pi/\lambda$ and d represents the unfolded path length). The expressions for the various coefficients can be found in [7-8].

The model developed in this paper launches rays that pass through the vertices of sphere B in Figure 2. Each ray then propagates in the environment and interacts with objects as they are encountered. The technique applied to find these ray-surface interactions is described in [9]. Propagation is terminated when the number of ray-object interactions reaches a defined limit. An array of tree structures is used to hold the geometric ray information.

To find ray paths from the transmitter to the receiver, the array of tree structures and the location of the receiver are used in conjunction with the angular test described in Figure 1b. Rays passing this test are deemed to arrive at the receiver and their complex field contribution is calculated using equation 1. In addition, for each ray the time of flight (delay) information and departure and arrival angles are calculated. Information such as path loss, K-factor, rms delay spread, rms azimuth spread and coherence bandwidth is calculated from the group of paths arriving at the receiver.

Traditionally, diffraction is difficult to include in a ray-launching model. The process requires re-launching of rays from each illuminated edge. In this paper a novel diffraction technique has been developed based on forward/backward ray launching from the transmitter/receiver respectively. Additional rays are launched from the transmitter and receiver to determine illuminated edges. Two further arrays are used to store the ray geometries. Using this data, all possible edge-

illuminating paths from the transmitter and receiver (up to the order specified by the user) are identified. If both the transmitter and receiver illuminate an edge then a possible diffracted path is found. To find the actual diffraction point, the method described in [10] is used. Using this method, all second order diffraction and multiple reflection-diffraction and diffraction-reflection ray paths are identified in a three dimensional space (including off-axis diffraction paths).

In this modelling work, irregular terrain is also taken into account. However, foliage attenuation is still under development and is not considered in this paper. A different approach is adopted to determine ray-terrain interaction. Small segments of the rays are compared with the terrain profile to determine if a ray intersection occurs.

3. MEASUREMENT SYSTEM AND SITE

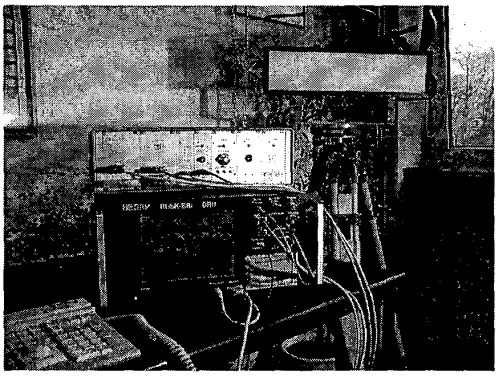

Figure 3: The MEDAV RUSK BRI channel sounder.

This section describes the channel sounding hardware (Figure 3) and the measurement campaign conducted to obtain site-specific validation data. The MEDAV channel sounder [11] supports far-field measurements at bandwidths of up to 120MHz. The unit currently operates in the 2GHz (UMTS, Bluetooth, IEEE802.11b) and 5GHz (Hiperlan/2 and IEEE802.11a) bands. The hardware is capable of resolving multipath components separated by 16ns in the time domain and 1-2 degrees in the space domain. Spatial separation is achieved using a super resolution ESPRIT algorithm in conjunction with an active 8-element receive array.

The measurement campaign for an urban environment was conducted in the city center of Bristol using a 20MHz segment of UMTS spectrum. In the prediction model, time resolution is reduced to around 100ns to reflect the band-limited transmission. Figure 4 shows a view of the city. The city is made up of densely packed buildings that are mainly constructed from stone and concrete. Most of the buildings are no more than 5 stories high, however there is a significant degree of dense foliage present in many locations. Significant terrain variation is also observed over the test site.

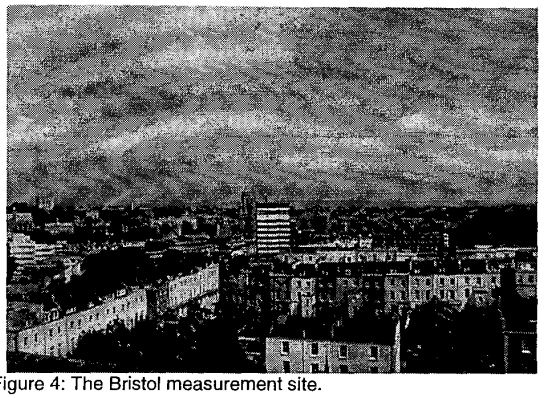

Figure 4: The Bristol measurement site.

4. PREDICTION RESULTS AND COMPARISON WITH MEASUREMENTS

Figure 5 shows the locations of the transmitter and receiver for the measurements used in the comparison.

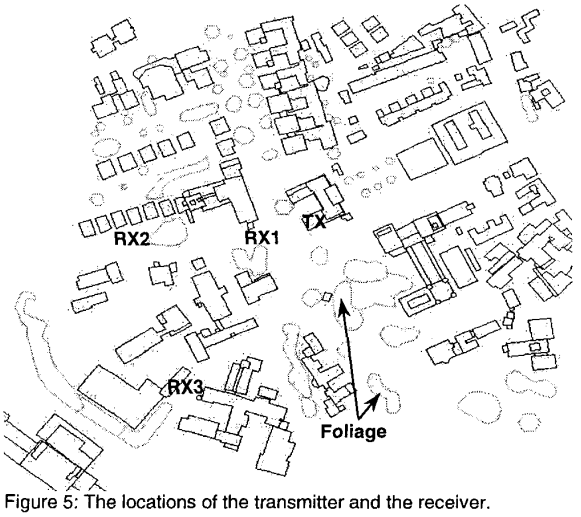

Figure 5: The locations of the transmitter and the receiver.

The building database was converted from the UK TWP Format for a three Dimensional Geographical Dataset [12]. Technical Working Parties (TWP) are sub-committees of the National Radio Propagation Committee (NRPC). The standard defines a detailed format for the collection of 3D building data, which is presented in drawing-interchange file format (DXF).

The predicted ray geometry for location RX3 is shown in Figure 6. During the measurement campaign, a dipole antenna was used at the transmitter while the receiver uses an isotropic antenna array with a beamwidth of 120 degrees in azimuth. The electric field pattern of these antennas is considered during the modelling process, as identified in equation (1).

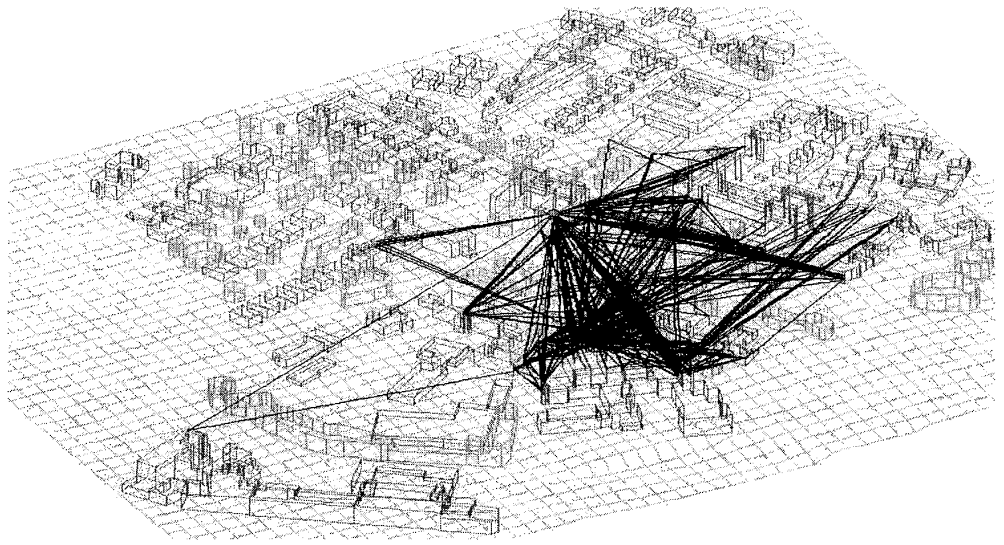

Figure 6: Predicted ray geometry at location RX3. Model settings: 1080 rays launched, 5 orders of reflection and 2 orders of diffraction considered.

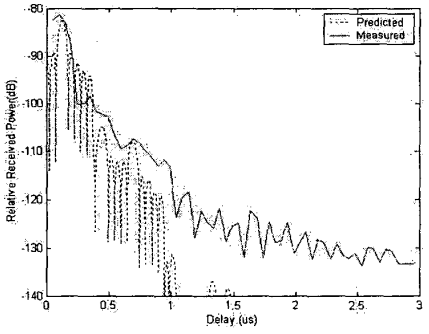

Figure 7: Predicted and measured power delay profile at location RX1. Predicted rms delay spread is 81.98ns, compared to 72.43ns measured.

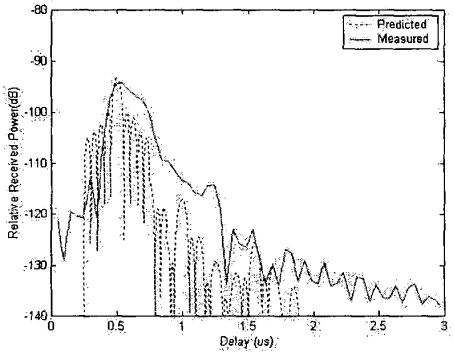

Figure 8: Predicted and measured power delay profile at location RX2. Predicted rms delay spread is 149.62ns, compared to 132.76ns measured.

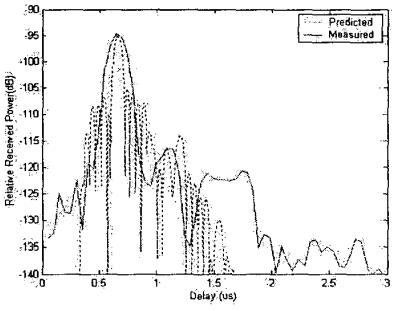

Figure 9: Predicted and measured power delay profile at location RX3. Predicted rms delay spread is 128.64ns, compared to 113.89ns measured.

The predicted results shown in Figures 7-9 were obtained using 5 orders of reflection and 2 orders of diffraction. The electric properties of materials in the environment are assumed to be uniform. The relative permittivity and conductivity were fixed at values of 5 and 0.005S/m respectively. These values were derived in [3] as optimum bulk parameters for an urban environment. The predicted results were band limited to 20 MHz to aid comparison.

The predicted power delay profile at all three RX locations compare well with those measured. Here, comparison of the instantaneous power delay profiles (PDP) is performed. It was shown in [2] that the shape of the PDP varies significantly for small displacements of the TX and/or RX (due to phase variation on a per ray basis). Since the ray model cannot accurately predict arrival phase, perfect agreement between measured and modelled instantaneous power delay profile cannot be

achieved. However, accurate prediction of the average power delay profile along a short route can be performed, as can the statistics of the power delay spectrum.

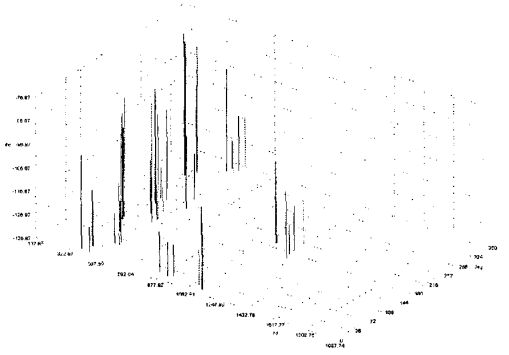

Figure 10: Example Delay Azimuth Profile predicted by the model.

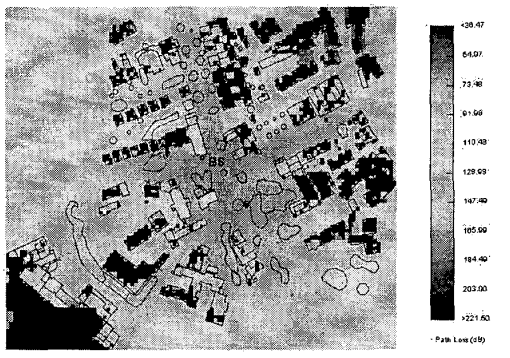

Figure 11: Signal coverage analysis by the model.

In addition to the prediction of power delay profiles, other types of channel characterization are possible. Figure 10 shows a delay azimuth profile and Figure 11 shows a signal coverage plot. Both results were produced using the settings described in Figure 6. The transmitter was placed at a height of 10m above the terrain at the location shown in Figure 11.

5. CONCLUSIONS

A new fully three dimensional propagation model for pico and microcellular environments has been introduced. The model predicts spatial and temporal channel information in addition to more traditional values such as field strength. Two key ray launching and detecting strategies were described and the method based on simple angle tests was chosen for further development. The ray launching technique has been extended to support multiple off-axis diffraction/reflection paths by performing forward /backward ray tracing from the transmitter/receiver respectively.

The properties and specifications of the Department's MEDAV channel sounder have been introduced and the urban measurement site described. Three locations were selected for comparison. The measured and predicted power delay profiles were compared and good agreement was obtained in terms of relative received power versus time of arrival.

The model is still under development and future work includes the modelling of foliage attenuation, the comparison of delay azimuth profiles and a detailed study of the model's indoor/outdoor prediction capabilities.

ACKNOWLEDGEMENTS

The authors would like to thank Dr Georgia Athanasiadou for her comments, support and advice during the first year of this project. BS Lee would also like to thank ORS for their financial support.

REFERENCES

[1] G.E. Athanasiadou, and A.R. Nix, "A Novel 3D Indoor Ray Tracing Propagation Model: The Path Generator and Evaluation of Narrow-Band and Wide-Band Predictions", IEEE Trans. Veh. Tech., vol. 49, pp.1152-1168, Jul 2000

[2] G.E. Athanasiadou, A.R. Nix, and J.P. McGeehan, "A Microcellular Ray-Tracing Propagation Model and Evaluation of its Narrow-Band and Wide-Band Predictions", IEEE Jour. On Selected Areas in Coms., vol. 18, pp.322-335, Mar. 2000

[3] G.E. Athanasiadou, A.R. Nix, and J.P. McGeehan, "Investigation into the sensitivity of a Microcellular Ray-Tracing Model and Comparison of the predictions with Narrowband Measurements", IEEE VTC, pp.870-874, May 1998

[4] E.K. Tameh, A.R. Nix and M.A. Beach, "A 3D Integrated Macro and Microcellular propagation model Based on the Use of Photogrammetric Terrain and Building Data", IEEE VTC, vol. 3, pp.1967-1961, 1997

[5] K.J. Gladstone, and J.P. McGeehan, "Computer Simulation of the Effect of Fading on a Quasi-Synchronous Sideband Diversity AM Mobile Radio Scheme", IEEE Jour. on Selected Areas in Coms., vol. 3, pp.191-203, Jan 1984

[6] H. Kenner, "Geodesic Math and How to Use it", Berkeley, CA: University of California Press Ltd., 1976

[7] J.H. Tarng, W.R. Chang, and B.J. Hsu, "Three-Dimensional Modelling of 900-MHz and 2.44-GHz Radio Propagation in Corridors", IEEE Trans. Veh. Tech., vol. 46, pp.519-527, May 1997

[8] R.G. Kouyoumjian, and P.H. Pathak, "A Uniform Geometrical Theory of Diffraction for an Edge in a Perfectly Conducting Surface", IEEE Proc., vol. 62, pp.1448-1461, Nov. 1974

[9] J.D. Foley, A. Dam, S.K. Feiner, J.F. Hughes, "Computer Graphics: Principles and Practice", Addison Wesley Publishing Company, 1996

[10] A.G. Kanatas, I.D. Kountouris, G.B. Kostaras, and P. Constantinou, "A UTD Propagation Model in Urban Microcellular Environements", IEEE Trans. Veh. Tech., vol. 46, pp.185-193, Feb 1997

[11] www.medav.de

[12] twp.dera.gov.uk